Creep and fluidity of a real granular packing near jamming

van Bau Nguyen, Thierry Darnige, Ary Bruand, Eric Clément

Creep and fluidity of a real granular packing near jamming

Van Bau Nguyen[1,2], *Thierry Darnige*[1], *Ary Bruand*[2], *Eric Clement*[1]
[1] *PMMH, ESPCI, CNRS (UMR 7636) and Univ. Paris 6 & Paris 7, 75005 Paris France.*
[2] *CNRS/INSU, ISTO (UMR 6113), Univ. Orleans, 45071 Orleans France.*
(Dated: January 10, 2011)

We study the internal dynamical processes taking place in a granular packing below yield stress. At all packing fractions and down to vanishingly low applied shear, a logarithmic creep is evidenced. The experiments are analyzed under the scope of a visco-elastic model introducing an internal "fluidity" variable. For all experiments, the creep dynamics can be rescaled onto a unique curve which displays jamming at the random-close-packing limit. At each packing fraction, a stress value is evidenced, corresponding to the onset of internal granular reorganisation leading to a slowing down the creep dynamics before the final yield.

PACS numbers: 47.57.Gc, 83.80.Fg, 65.60.+a

For granular matter, it is currently accepted that a quasi-static limit exists as for grains of macroscopic size, thermally activated processes can be ignored. Therefore, at low shear rate, mechanical properties of granular packing are usually described phenomenologically by rate independant constitutive relations [1]. However, there are compelling experimental evidences that for granular in "real" environmental conditions (i.e. finite temperature or background noise), this limit is just a short-time approximation and time dependent processes are significant on the long run. In soil mechanics and engineering, where the issue of long time resistance to stress is of practical importance, standart tests have displayed aging properties for a large class of granular materials [2]. Other experiments have pointed out the central importance of nanometric scales where humidity and/or contact plasticity [3, 4] do impact significantly the macroscopic behavior. Recently, it has been shown how tiny thermal variations may drive important packing reorganizations [5, 6]. Since the original proposition of "soft glassy rheology" made by Sollich et al.[11] various models tried to capture the complex energy reorganization dynamics taking place in weak amorphous solids or yield-stress fluids in relation with rheological constitutive laws. The rate of stress relaxation is often described phenomemologicaly by an internal variable called "fluidity" [12, 13]. Recent theoretical developments suited to explain microscopically the emergence of plasticity, have proposed a simple picture where localized elastic instabilities release irreversibly long range elastic constraints [9] organized spatially as avalanches driven by shear rate [10]. For granular material suppositely belonging to this class of problems, many numerical simulations were done, based on soft interparticular interactions [14]. These studies have brought to the front the idea of an "universal" jamming transition scenario based on the onset of mechanical rigidity (see a recent review and refs in ([15])). Interparticle solid friction present in real granular packing was shown to affect the rigidity onset [16] and stabilize packing at compacity below the random close packing limit. Importantly, solid friction is related to surface roughness and contact plasticity, both taking place at a sub-granular scale where the exact role of thermal activation[5, 6] or mechanical external noise [7, 8] is to a large extend, an open and challenging issue.

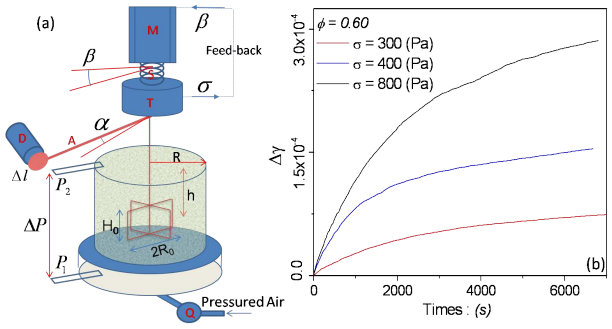

FIG. 1: (a)Schematics of the shear cell. (M): motor, (S): torsion spring, (T): torque probe, (D): induction distance probe, (A): transversal arm, (Q): flowmeter, P_1: differential pressure probes. (b) Creep deformation : $\Delta\gamma(t)$ under constant shear at packing fraction $\phi = 0.60$.

In this paper, we explore systematically this question by studying the creeping properties a constant shear of a granular packing, in order to reveal and characterize the internal relaxation processes.

The experiments are suited to perform mechanical tests on granular packing at well defined packing fractions ϕ (see fig.1) and to this purpose, the set-up is designed as an air fluidized bed. The container is a plastic cylinder of inner diameter $D = 10cm$ closed at its bottom by a metal grid supported by a honeycomb grid. Pressured air is introduced in an admission chamber below the grid at a controlled over-pressure ΔP. We use glass beads of density $\rho = 2500kg/m^3$ and mean diameter $d = 200\mu m$ (R.M.S. polydispersity $\Delta d = 30\mu m$). A mass M of grains is poured into the container such that the typical packing height is $L = 10cm$. Using a flow rate right above the fluidization value, we obtain after stoppage, an initially loose granular packing at a compacity $\phi \approx 0.56$. Then,

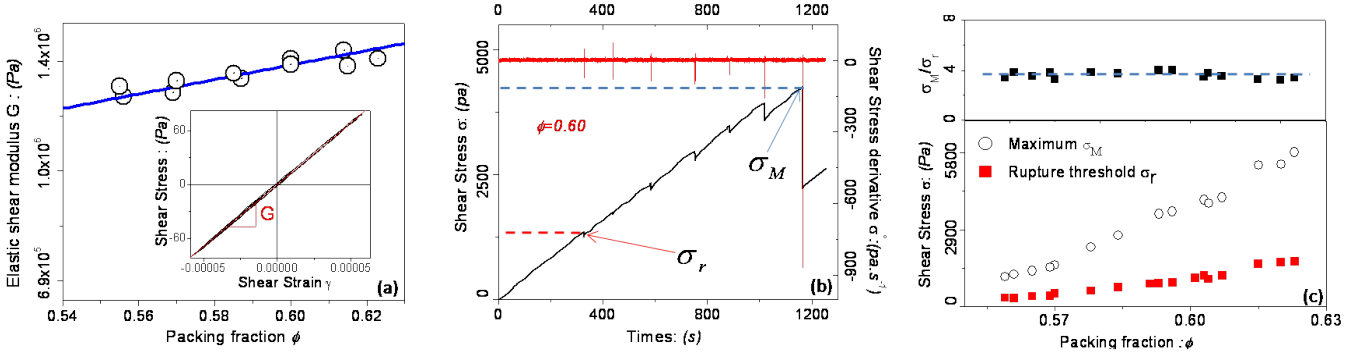

FIG. 2: . (a) Shear modulus $G(\phi)$ under gravity confinement. Straight line $y = G_0 x$, with $G_0 = 2,28.10^6\ Pa$. (b) Response to a stress ramp : shear stress σ as a function time for $\dot{\beta} = 0.00104\ rd/s$ and a packing fraction $\phi = 0.6$. First rupture stress σ_r and maximal stress σ_M are displayed as horizontal dotted lines. (b) For the same rotation rate, σ_r, σ_M and the ratio $\frac{\sigma_M}{\sigma_r}$ as a function of packing fraction.

by successive tapping on the container side, the packing fraction can be increased up to the desired packing fraction (maximal value $\phi = 0.625$). Before each mechanical measurement, the packing fraction value is evaluated from a linear fit between pressure drop ΔP and flow rate Q : $\Delta P = \kappa Q$, stemming from Darcy's law. The relation between permeability K and packing fraction was calibrated by preliminar series of experiments and a Carman-Kozeny relation [18] was obtained : $K(\phi) = A\frac{(1-\phi)^3}{\phi^2}d^2$, with $A = 1/165$. Consequently, packing fraction is determined through the relation : $K(\phi)\ \phi = \eta\frac{4}{\kappa\pi}\frac{M}{D^2\rho}$. To shear the granular packing, we use a four blades vane of height $H_0 = 2.54cm$ and diameter $2R_0 = 2.54cm$ (see fig.1(a)),introduced at a depth $h = 5cm$ below the surface prior to the initial fluidization process. This procedure creates initially reproducible conditions for shear at fixed packing fraction. Shear stress is applied through the vane (see fig.1) connected axially to a torque probe *(T)* itself coupled to a brushless motor *(M)* via a torsion spring *(S)*. The vane rotation angle α is monitored via a transversal arm *(A)* which rotation is followed by a displacement induction probe *(D)*. The motor rotation angle β can be imposed at a $2\pi/10000$ precision. Torque and displacement signals as well the motor command, are connected to a Labview controler board programed to impose a motor rotation rate or a fixed stresse using a feedback loop on the torque signal. In the following, we ignore the stress and strain spatial distribution, due to the Couette cell geometry and define only average values obtained from mesurements of angular rotation α and torque T. The mean packing deformation γ is defined as $\gamma = \frac{\alpha R_0}{R-R_0}$ and the mean shear deformation is : $\sigma = \frac{T}{2\pi R^2 H_0}$. On fig.1(b), we display three examples of creep curves $\Delta\gamma(t) = \gamma(t) - \gamma(0)$ obtained at fixed compacity and shear stress values σ.

Elastic response - To obtain the elastic response of the packing initially prepared at a given packing fraction, stress cycles were performed corresponding to sinusoidal deformations at small amplitudes around 10^{-5}. The cycles are done under constant mean confining pressure (hydrostatic loading) $P_0 = \rho\phi g h$. In the short time limit, the response is essentially reversible (see inset of fig.(2(a)). The effective elastic shear modulus increases with packing fraction. Mean-field Hertz elasticity theory (see[17] and refs inside), under a confining pressure P_0 would yield a shear modulus scaling as $G_{eff} \propto E_0\,(\phi Z)^{2/3}\left(\frac{P_0}{E_0}\right)^{1/3}$, where Z is the mean contact number and E_0 the material Young's modulus. Thus, one should obtain a linear relation : $G_{eff} = G_0\phi$, which correspond to our experimental finding (see line on figure 2(a)) with a value of $G_0 = 2,28.10^6 Pa$.

Response to a stress ramp - To identify the the maximal stress supported by the packing before yield, shear stress ramps were applied at a constant motor rotation rate ($\dot{\beta}$), using the softest spring constant available ($k = 2,45.10^{-3} Nm/rd$). On figure 2(a), the stress response at $\phi = 0.60$ is displayed as a function of time. At first, a linear increase of the stress is observed with a slope corresponding to the spring constant. Then, at a given stress level σ_r, we observe the emergence of well marked and sudden granular material reorganizations (see top view on fig.2(b)) in the form of rather equidistant events corresponding to stress drops and large plastic deformations ($\delta\gamma = 10^{-3} - 10^{-2}$). We define this stress value as the "first rupture stress" : σ_r. However, stress can still be increased up to a maximal value σ_M where a large stress jump is evidenced and a subsequent stick-slip dynamics is observed. This final stress value corresponds to a Coulomb yield criterion as we verified that its value increases linearly with the confining pressure. Such experiments were performed varying packing fraction and ramp velocities and we only display here, stresses obtained at the slowest driving velocity where the values are quite insensitive to the rotation rate. On fig 2(b), the rupture, maximal and dynamical stresses are displayed as a function of packing fraction for a rotation rate ($\dot{\beta} = 0.00104 rd/s$). The values increase strongly

with packing fraction possibly from a vanishing value situated around 0.52. Interestingly these stress values are strongly related since their ratio stay constant with packing fraction: $X = \sigma_M/\sigma_r = 3.5 \pm 0.2$ (see upper part of fig.(2(b)).

Creep flow - This part is concerned with the creep

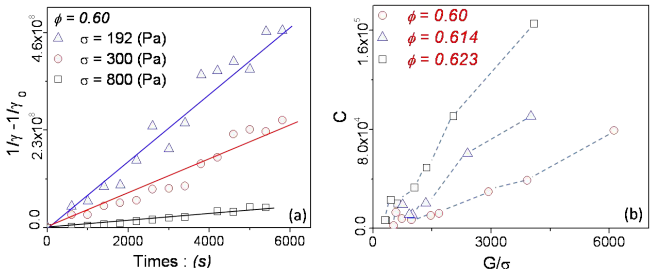

FIG. 3: Creep experience. (a) plot of $\dot{\gamma}^{-1} - \dot{\gamma}_0^{-1}$ as a function of time for creep experiments performed a constant packing fraction $\phi = 0.6$ for various shear stresses, the straight lines are linear fits : $y = Ct$. (b) Values of the fitted slopes C as a function of $G(\phi)/\sigma$ for three values of packing fractions.

response of the granular packing under constant shear stress, changing the packing fraction between 0.56 and 0.625. The procedure consists of two steps: first a monotonic loading up to the desired stress value. This initial step is fast with respect to the creep dynamics : typically less than $200s$ at the slowest motor rotation velocity. We verified that the loading time, is much smaller than the inverse of the observed initial shearing rate. Then, a feed back procedure is programed on Labview is to control at less than 1% the stress value σ. The onset on feed-back defines the initial time $t = 0$. For all experiments, we observea slow increase of the deformation $\Delta\gamma(t)$ (see fig. (1b). The creep dynamics increases with the applied shear stress and a decreases for large values of the packing fraction. From the creep curves, strain rate is computed for a time step $\delta t = 1s$. From time to time, to keep the shear stress constant in the specified range, the motor angle changes abruptly. Consequently a strain rate acceleration is observed, followed by a decay down to the value before the jump, in less than $20s$. These phases were removed from the susequent analysis. On fig.3(a), we represent $\dot{\gamma}^{-1} - \dot{\gamma}_0^{-1}$ as a function of time for a fixed packing fraction at different applied shear stresses. Shear rate were averaged over a time window of $\Delta T = 400s$. We observe in all cases, a relation $\dot{\gamma}^{-1} - \dot{\gamma}_0^{-1} = Ct$, corresponding to a long time logarithmic creep $\gamma = \gamma_0 + \frac{\dot{\gamma}_0}{C}\ln(1 + Ct)$. On fig. (3b), we represent the values of C extracted from a linear fit as a function of $G(\phi)/\sigma$ and this, for different packing fraction values. We observe a monotonic increase, more prononced at larger packing fraction.

Rheological model - To analyze quantitatively the data, we use a theoretical model proposed by Derec et al.[12] in the context of complex fluids rheology. We propose

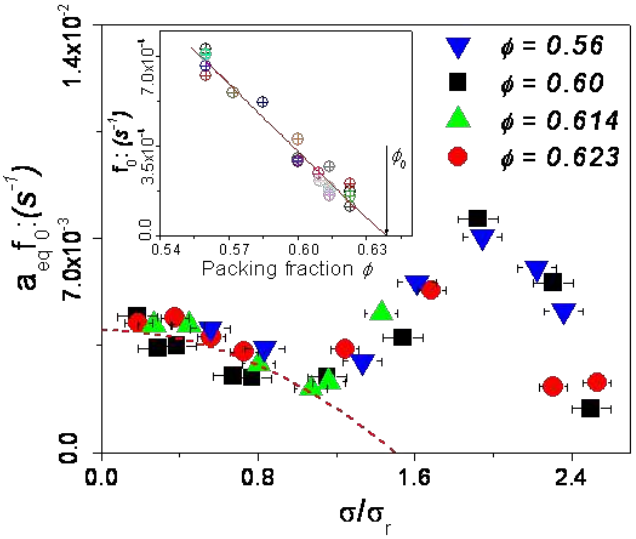

FIG. 4: Rescaled aging parameter $a_{eq}f_0$ as function of rescaled of shear stress $\frac{\sigma}{\sigma_r}$, dotted line: $y = \frac{1}{t_*}\left(1 - (\frac{x}{1.5})^2\right)$ with $t_* \cong 250s$. Inset : initial fluidity f_0 as a function of packing fraction, for different shear stresses, fit line: $y = F(\phi_0 - \phi)$ with $F = 0.0086$ and $\phi_0 = 0.635 \pm 0.002$.

here to adapt it to the creep flows of granular packing. This model introduces an internal phenomenological variable called "fluidity" f which physical interpretation is simple as, it represents a time dependant rate of stress relaxation. It extends naturally the standart Maxwell visco-elastic rheology. As originally discussed by Derec et al.[12], the fluidity dynamics results from the simplest and lowest order coupling involving natural aging and stress rejuvenation. The set of coupled dynamical equations are :

$$\partial_t \sigma = -f\sigma + G\dot{\gamma} \quad (1)$$

$$\partial_t f = -af^2 + r\dot{\gamma}^2 \quad (2)$$

parameter a is the aging parameter and r the shear rate induced rejuvenation parameter. At constant shear stress σ, one obtains the relation $f\sigma = G\dot{\gamma}$ thus yielding : $\partial_t f = -a(1 - (\frac{\sigma}{\sigma_D})^2)f^2$, where $\sigma_D = \sqrt{a/r}$ is the dynamical shear corresponding to steady shear rate and steady fluidity. The solution of this equation is then : $f(t) = \frac{f_0}{1 + a_{eq}t}$, introducing an equivalent aging parameter :

$$a_{eq} = a(1 - (\frac{\sigma}{\sigma_D})^2) \quad (3)$$

The shear rate variation is then : $\frac{1}{\dot{\gamma}} - \frac{1}{\dot{\gamma}_0} = \frac{G}{\sigma}a_{eq}.t$. This relation leads to a long time logarithmic creep as observed experimentally. Moreover, the experimental slopes C of fig. (3b) can be identifed using the relation:

$$a_{eq} = C.\frac{\sigma}{G} \quad (4)$$

For all experiments performed at different stresses and packing fractions, the initial fluidity value f_0 =

$G(\phi)\dot{\gamma_0}/\sigma$, can be plotted as a function of ϕ. For all stresses, data collapse onto a quasi-linear curve (see inset of fig.(4)); the denser is the packing, the lesser is initial fluidity. The linear extrapolation of this curve to $f_0 = 0$ yields a value $\phi_0 = 0.635 \pm 0.002$, close to random close packing of monodisperse sheres. This can be interpreted as a arrest of the creep dynamics at a packing fraction corresponding to the jamming limit for a random assembly of frictionless spheres [19]. Furthermore, the aging dynamics can be characterized by computing the equivalent aging parameter a_{eq} according to relation (4) If a and r are independant of shear, a_{eq} should decrease quadratically and reach a zero value at a finite stress corresponding to the dynamical stress σ_D according to relation 3. We realized that aging parameter and initial fluidity where not independent and to characterize the aging properies we plot on fig.(4), $Y = f_0 a_{eq}$ as a function of the adimensionalized stress : $X = \sigma/\sigma_r$. The striking feature is that all data collapse onto a single curve for the whole range of stresses and packing fractions studied. The second important feature is that a_{eq} displays a non monotonic behaviour with a minimum value at $\sigma \approx \sigma_r$ ($X = 1$) corresponding to the onset of the strain rate bursts identified in the stress-ramp experiments. This behavior is clearly the signature of internal granular reorganizations which leads to a slowing down of the creep dynamics instead of an increase as one might expect when shear is increased. For values above $X \approx 2$, the creep dynamics increases again before reaching the dynamical stress threshold ($a_{eq} = 0$) at $\sigma_D \approx 2.4\sigma_r$. For smaller values of shear stress, i.e. below σ_r, the predictions of Derec's model (see relation (3)) can still be validated with a dynamical stress $\sigma_D = 1.5\sigma_r$ (see dashed line on fig. (4)). However, from a phenomenological point of view there is clearly an effect missing and it would be interesting to see in furter developments of the fluidity theories, how such a behavior may be accounted for by extra terms in the fluidity equation. By extrapolation it appears that aging is still present in the limit of zero applied shear stress.

This experimental study shows that down to vanishing low applied shear and up to the yield stress value, internal relaxation processes are present in a granular packing. The logarithmic creep hence evidenced, was analyzed under the scope of a simple visco-elastic model introducing a time dependent rate of relaxation (the fluidity). The dynamics can be viewed as a competition beween intrinsic aging and stress rejuvenation. The model allows a dynamical characterization of the initial packing fluidity which is shown to decrease linearly with packing fraction and vanish at the random close packing limit. However, under finite stress, we identified the onset of major internal reorganizations, slowing down the creep process and setting the yield stress to higher values. This process could be related to the onset of stress induced anisotropy [20, 21] or shear band formation. In this work, we show that the inherent fragility of granular matter under shear can be put in perspective with creep properties evidenced in a large class of yield stress fluids [23]. This internal dynamic is the sign of a peculiar fragility for this type of solid, possibly mediated by thermal activation or by background mechanical noise. However, it may also be intrinsically related to the nature of elastic instabilities leading to the plastic response in amorphous solids [10], which may render amorphous solids especialy fragile under finite shear [24].

Acknowledgement - We thank the CNRS-PEPS program, the "Region-Centre" and the ANR "Jamvibe-2010" for their financial support.

[1] D.M.Wood, *Soil Behaviour and Critical State Soil Mechanics*, Cambridge University Press (Cambridge, 1990).
[2] J.H. Schmertmann, J.Geotech.Eng.**117**, 288(1991).
[3] L.Bocquet et al., Nature **396**, 735 (1998).
[4] G.Ovarlez, E.Clement, Pys.Rev. E **68**, 031302 (2003).
[5] K. Chen et al., Nature **442**, 257 (2006).
[6] T.Divoux, H. Gayvallet and J.-Ch. Geminard, Phys. Rev. Lett. **101** 148308 (2008).
[7] P.A. Johnson et al. Nature, **451**, 47 (2008).
[8] G.A. Caballero-Robledo and E. Clement, Eur.Phys.J.E **30**, 395(2009).
[9] G. Picard et al. Eur.Phys.J.E **15**371(2004); A.Tanguy et al. Eur.Phys.J.E **20**, 355 (2006); C. Maloney and A. Lemaitre, Phys.Rev.E **74**, 016118 (2006).
[10] A. Lemaitre et C. Caroli, Phys. Rev. Lett., **103**, 065501 (2009); S.Karmakar, E.Lerner, I.Procaccia, Phys.Rev.E, 055103(R). (2010).
[11] P.Sollich et al., Phys. Rev. Lett. **78**, 2020 (1997).
[12] C.Derec, A.Adjari and F.Lequeux Eur.Phys.J.E **4**, 395(2001).
[13] L.Bocquet, A.Colin, A.Ajdari, Phys. Rev. Lett. **103**, 036001 (2009).
[14] C.O'Hern et al. Phys.Rev. E **68** 011306(2003).
[15] M van Hecke J.Phys.: Cond.Matt. **22** 033101 (2010).
[16] E.Somfai et al. Phys. Rev. E **75** 020301(R)(2007).
[17] H.Makse et al. Phys.Rev.E **70**, 061302 (2005).
[18] J.Bear, *Dynamics of Fluids in Porous Media*, Dover (1989).
[19] S.Torquato and F.H.Stillinger, Rev.Mod.Phys. **82**,2633 (2010).
[20] J.Geng et al. Physica D **182**, 274 (2003); Atman et al., Eur.Phys.J.E **17**, 93(2005).
[21] Y.Khidas and X.Jia, Phys. Rev. E **81**, 021303 (2010).
[22] M.Tsamados, Eur.Phys.J.E **32**, 165(2010); H.G.E.Hentschel et al., Phys.Rev. Lett.,**104** 025501 (2010).
[23] F.Caton and C.Baravian, Rheologica Acta. **47**, 601, (2008).
[24] H.G.E.Hentschel et al., *Do athermal amorphous solids exist?,* Cond Mat-1101.0101v1 (2010).